Non-Linear robust control optimization to improving the aerodynamics in gas turbine

Optimisation d'un contrôle robuste non linéaire pour améliorer l'aérodynamique de la turbine à gaz

Abdesselam Debbah*[1,2], Hamid Kherfane[1] & Mahieddine Berkani[3]

[1]L2RCS Laboratory, Department of Electronics, University of Badji Mokhtar, Po Box 12, 23000, Annaba, Algeria.
[2]Department of Petrochemical and Process Engineering, University of 20 Aout 1955, Skikda, 21000, Algeria.
[3]Departement of Electromechanical, University of Badji Mokhtar, Po Box 12, Annaba, 23000, Algeria.

Article Info

Article history:

Received :12/09/2018
Revised :22/04/2019
Accepted: 09/09/2019

Keywords

Gas turbine, Surge-Rotating stall, Robust control, Constrained Genetic algorithm (GA).

ABSTRACT

This paper presents a novel robust approach to control the aerodynamics instabilities, surge and rotating stall of a Variable Speed Axial Compressor (VSAC) in gas turbine process. The used model to design the controller is Egeland-Gravdahl who has been commonly recognized as standard when reporting some bifurcation behavior of VSAC which cannot be captured by constant-speed models. The proposed non-linear robust control is reformulated as an optimization problem, the first reformulation is linear matrix inequality (LMI) solved by interior point optimization algorithm, the second reformulation is non-linear constrained optimization solved by genetic algorithm (GA).The two optimization approaches are tested and compared using Matlab software. Promising simulation results were obtained for both optimization approaches, but the robust controller based on genetic algorithm optimization presents better performances to tackle a restricted specification and operating conditions.

Mots clés

Turbine à gaz , Pompage-Décrochage tournant, Commande robuste , Algorithme génétique contraint (AG).

RESUME

Cet article présente une nouvelle approche robuste pour contrôler les instabilités aérodynamiques, le pompage et le décrochage tournant d'un compresseur axial à vitesse variable (VSAC) au niveau d'une turbine à gaz. Le modèle utilisé pour concevoir le contrôleur est Egeland-Gravdahl, qui est reconnu comme le modèle standard qui représente certains comportements de bifurcation, qui ne peuvent pas être représenté par des modèles à vitesse constante. La commande robuste non linéaire proposée est reformulée comme un problème d'optimisation : la première reformulation est l'inégalité linéaire matricielle (LMI) résolue par l'algorithme d'optimisation du point intérieur ; la seconde est une optimisation non linéaire sous contraintes résolue par l'algorithme génétique (GA). Les deux approches d'optimisation sont testées et comparées à l'aide du logiciel Matlab. Des résultats de simulation prometteurs ont été obtenus pour les deux approches d'optimisation. Cependant, le contrôleur robuste basé sur l'optimisation de l'algorithme génétique présente de meilleures performances en présences des spécifications et des conditions de fonctionnement restreintes.

Corresponding Author:
Abdesselam Debbah
L2RCS Laboratory, Department of Electronics, Departement of electronics,
University of Badji Mokhtar, Po Box 12, Annaba, 23000, Algeria.
Department of Petrochemical and Process Engineering, University of 20 Aout 1955, Skikda, 21000, Algeria.
Email: a.debbah@univ-skikda.dz

1. INTRODUCTION

Gas turbines are internal combustion engines, which require pressurized air, and are widely used in industrial and aeronautic applications. The pressurized air is delivered by air compressors suffering from two kinds of aerodynamic instabilities, namely, surge and rotating stall. These instabilities are deeply affected by speed dynamics. Indeed, speed transitions develop temporary rotating stall and cause a pressure drop in the output. [1]. Despite reported achievements in several papers [2],[4],[5],[9-13],[17],[18], devoted on stabilizing axial compressors being based on the constant speed assumption, or surge control only, or both surge and rotating stall, this paper tackles the simultaneous control of speed and instabilities (surge and rotating stall) in variable speed, using the most appeared and representative actuators closed control valve (CCV) and throttle valve, which it has remained an open problem [4],[17]. Contrary to Egeland-Gravdahl variable speed model, Moore-Greitzer original model does not imply any rotating stall development, since the working point is situated by an adequate margin to surge line. This temporary stall development and pressure drop can cause trouble for the normal turbo machines operation [4]. Experiment results are very important to study the gas turbine performances, but the high cost, test facilities and risks in test make the experiments so difficult [18],[19]. So, it is significant to make an early theoretical search with a very representative model as used in this work. In this paper, it has important to take Egeland-Gravdahl representation as model, due to its capacity to reporting some bifurcation behavior of Variable Speed Axial Compressors (VSAC).The first investigation on qualitative behavior of Egeland-Gravdahl non-constant speed model was first proposed by Sari et al. in [3]. Based on the results found in [4],[12],[13],[28], this paper investigates not only in the behavior of variable speed but also the behavior of the actuators [25],[29], especially the torque of the turbine and the valve throttle. Through a quantitative analysis of model, we note the sensitivity of bifurcation point (throttle valve) and its stability to the change of acceleration rates and desired speeds. Consequently, we have proposed an optimized state feedback control, subjected to different constraints, leads to a proved feasibility condition on the stability achieved for bounded disturbances and uncertainties, probably made the proposed strategy correctly in the case of practical experiments, who make the problem even more challenging [4],[1], and it is a new search hot point [18]. This paper wants to provide:

- An adapted linear matrix inequality (LMI) optimization based on non-linear control. It gives the application on a bifurcation nonlinear system.
- New key condition called in this paper Variable Speed Instabilities Constraints. It's the result of the bifurcation analysis depicted for two different acceleration rates and desired speeds.
- An adapted formulation of Genetic algorithm (GA) optimized nonlinear control, based on Lyapunov function, taking on consideration the non-linear function and constraints.

Unlike other optimization approaches, GA algorithm is based on the populations representing the different solutions for the optimization problem. These properties of mentioned algorithm result in improvement of the search ability and increasing the quickness of finding the optimum solution [27]. Since the constrained genetic algorithm, on-line LMI and off-line are supposed to find a solution to a given objective function but employ different strategies and computational effort, it is appropriate to compare their performance [18]. The paper is organized in seven principal sections. The Egeland-Gravdahl model and bifurcation model is presented in Section 2. Section 3 shows non-linear robust design. Section 4 describes constrained genetic algorithm optimized non-linear robust design. Section 5 shows the simulations results. Section 6, concludes with summary and discussion on the potential use of the proposed approaches on experimental test.

2. EGELAND-GRAVDAHL MODEL AND BIFURCATION ANALYSIS

A complete bifurcation analysis of the variable Speed Axial compressor model is carried out in this section. The Egeland-Gravdahl's model can be expressed as ordinary differential equations as below [2]:

$$\frac{d\Phi}{d\zeta}=\frac{H}{l_c(U)}\left[-\frac{\Psi-\psi_{c0}}{H}+1+\frac{3}{2}\left(\frac{\Phi}{W}-1\right)\left(1-\frac{J_1}{2}\right)-\frac{1}{2}\left(\frac{\Phi}{W}-1\right)^3-\frac{1}{\gamma_v^2}\left(\frac{\Phi^2}{H}+\frac{W^2J_1}{2H}\right)-\frac{U_d\Lambda_1\Gamma_E\Phi}{bH}\right] \quad (1)$$

$$\frac{dJ_n}{d\zeta}=J_n\left[1-\left(\frac{\Phi}{W}-1\right)^2-\frac{J_n}{4}-\frac{\mu n^2W}{3aH}-\frac{2U_d\Lambda_1\Gamma(m-1)W}{3Hbn}-\frac{4\Phi W}{3H\gamma_v^2}\right]\frac{3aHn}{(n-m_U(U)a)W} \quad (2)$$

$$\frac{d\Psi}{d\zeta}=\frac{\Lambda_2 b}{U}(\Phi-\Phi_T)-2\Lambda_1\Gamma\frac{U}{b}\Psi \quad (3)$$

$$\frac{dU}{d\zeta}=\Lambda_1\Gamma\frac{U^2}{b} \quad (4)$$

Matcont continuation and bifurcation software [6] are used to conduct the computations, and relevant parameters of the system model are given in (Tab. 2). The computed bifurcation diagram, for mass flow Φ and first harmonic of rotating stall with varying throttle parameter γ_T, for the cases $U_d = 65m/s$ and $U_d = 90m/s$ is presented. Figure.1 shows one of the bifurcation diagrams of the model where equilibrium of a constant and non-constant speed axial compression system are depicted as a function of throttle gain γ_T (Bifurcation Parameter). $\phi_T(\psi) = \gamma_T\sqrt{\psi}$ is known as the steady state compressor map which represents nonlinear relationship between the pressure rise at the output of the compressor and the mass flow. Figure.1 contains information about all steady states, and their stability, and identifies bifurcation points (BP) where steady states exchange stability, and new steady states are created or existing steady states disappear. The subcritical bifurcation point (BP) represents the peak value of pressure rise where the axisymmetric flow loses stability. Limit cycles originating from Hopf bifurcation point H (inferior) represent classical surge with J>0. Classic surge cycles occur only for an arrow range of values of the throttle parameter γ_T, and are therefore plotted separately in Figure 1.b).d).f).h).k) on a different parameters axis scale. Limit cycles from Hopf point H (superior) are not plotted because they are found to have negative J and are therefore nonphysical. Bifurcation diagrams, such as that in Figure 1, can be used to identify parameter regions of different global stabilities behavior [7]. In order to study the effects of speed variations on the system behavior, a simple proportional speed controller of the form $\Gamma_t = K_s(U_d - U)$, with U_d is the desired velocity of the wheel and K_s is a gain defining the rate of the acceleration.

Higher (lower) leads to faster (slower) rates of speed variations. Figure 1.e),f),g),h),i),k), which is depicted for two different acceleration rates and desired speeds, shows that the variation of the acceleration rate changes the bifurcation points over the physical limits $max(\gamma_T) = 1$, which can causes infeasibility of control law. The modification of manifolds form can change the behavior of the system in different ways, including the type and the range of instabilities and the relevant domain of attractions as well. The system behavior in the interval between the limit point (LP) and the bifurcation point (BP), takes on a considerable importance. The deformation also indicates that the amplitude of fully developed stall and the amplitude of the limit cycles corresponding to surges vary due the acceleration rate variations.

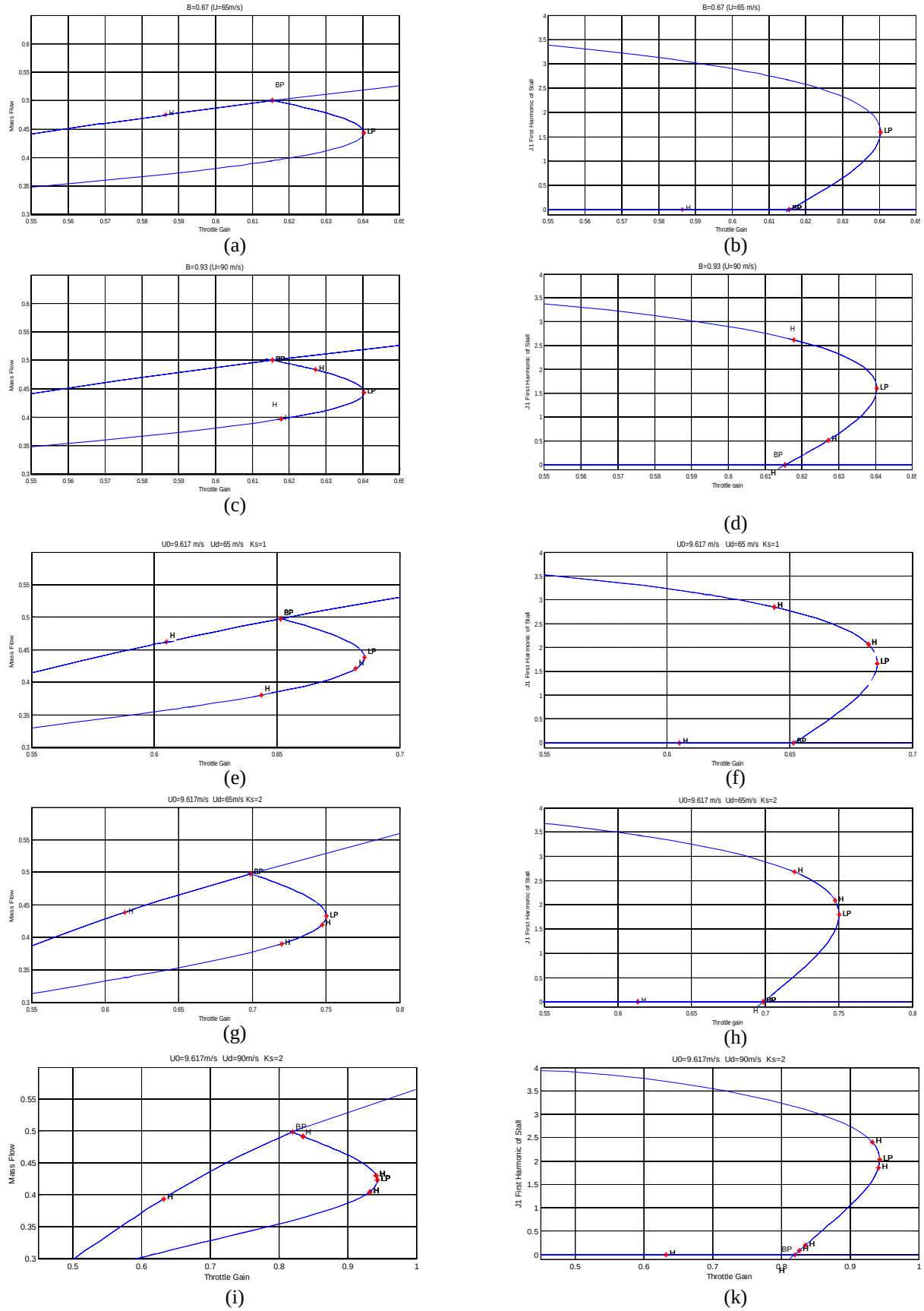

Figure 1. The bifurcation Analysis. (a),(b),(c),(d): Constant Speed behavior, (e),(f),(g),(h),(i),(k): Variable Speed behavior with Bolds lines show stable and dashed lines show unstable manifolds.

3. NON-LINEAR ROBUST CONTROL DESIGN

Gravdahl developed a model for variable speed axial compressors and considered the speed of the rotor as a state variable [2]. Later, Zaiet et al. [8] modified the model to include the pressure drop over a CCV and to make it suitable for control applications.

$$\frac{d\phi}{d\zeta}=\frac{H}{l_c(U)}\left[-\frac{\psi+\Psi_0-\psi_{c0}}{H}+1+\frac{3}{2}\left(\frac{\phi+\Phi_0}{W}-1\right)\left(1-\frac{J_1}{2}\right)-\frac{1}{2}\left(\frac{\phi+\Phi_0}{W}-1\right)^3-\frac{u_1}{H}-\frac{1}{\gamma_v^2}C_1J_1\right.$$
$$\left.-G_1(\phi+\Phi_0)u_3+G_1c(\phi+\Phi_0)^3+\Delta_\psi\right] \quad (5)$$

$$\frac{dJ_1}{d\zeta}=J_1\left[1-\left(\frac{\phi+\Phi_0}{W}-1\right)^2-\frac{J_1}{4}-G_2-G_3u_3+G_3c(\phi+\Phi_0)^2-\frac{1}{\gamma^2}C_2(\phi+\Phi_0)\right]\frac{3aH}{(1-m_U(U)a)W} \quad (6)$$

$$\frac{d\psi}{d\zeta}=\frac{\Lambda_2}{U+U_0}\left(\phi+\Phi_0-u_2\sqrt{\Psi}\right)-2\Lambda_1\frac{U+U_0}{b}(\psi+\Psi_0)u_3+2\Lambda_1\frac{U+U_0}{b}(\psi+\Psi_0)c(\phi+\Phi_0)^2-\Delta_\phi \quad (7)$$

$$\frac{dU}{d\zeta}=\Lambda_1(U+U_0)^2u_3-\Lambda_1(U+U_0)^2c(\phi+\Phi_0)^2 \quad (8)$$

with

$$l_c(U)=l_l+l_E\frac{U_d}{U}+\frac{1}{a},\ C_1=\frac{W^2}{2H},\ C_2=\frac{4W}{3H},\ G_1=\frac{U_0\Lambda_1l_E}{bH},\ G_2=\frac{\mu W}{3aH},G_3=\frac{2U_0\Lambda_1\Gamma(m-1)W}{3Hb} \quad (9)$$

Let us consider the model (5,6,7,8) as:

$$\dot{x}=f(\zeta,J_1,\Phi,\Psi,U,u) \quad (10)$$

where f is a continuously differentiable nonlinear function, with the state variables $x=(J_1,\Phi,\Psi,U)$ belongs to R^4.The actuators forces are input variables u1, u2 and u3 defined respectively as the pressure drop over CCV, the throttle gain, and the non-dimensional drive torque being used to increase the speed.

3.1. Control design

Let us consider the following control effort that can stabilize the system the nonlinear system (10) in error coordinates [13]:

$$u_1=-\psi-\Psi_0+\psi_{c0}+H+\frac{3H}{2}\left(\frac{\phi+\Phi_0}{W}-1\right)-\frac{H}{2}\left(\frac{\phi+\Phi_0}{W}-1\right)^3+G_1H(\phi+\Phi_0)K_3U+l_cK_1\phi$$

(11)

$$u_2=\frac{\phi+\Phi_0}{\sqrt{\psi+\Psi_0}}+\frac{2\Lambda_1\sqrt{\psi+\Psi_0}(U+U_0)^2}{\Lambda_2}K_3U+\frac{1}{\sqrt{\psi+\Psi_0}}K_2\psi \quad (12)$$

$$u_3=c(\phi+\Phi_0)^2-K_3U \quad (13)$$

The system (10) can be written

$$\frac{d\phi}{d\zeta}=-K_1\phi+\delta_1 \quad (14)$$

$$\frac{dJ_1}{d\zeta}=f_{J1}(J_1,\phi,\psi,U)=J_1\left[1-\left(\frac{\phi+\Phi_0}{W}-1\right)^2-\frac{J_1}{4}-G_2-G_3u_3+G_3c(\phi+\Phi_0)^2-\frac{1}{\gamma^2}C_2(\phi+\Phi_0)\right]\frac{3aH}{(1-m_U(U)a)W}$$

(15)

$$\frac{d\psi}{d\zeta}=\frac{\Lambda_2}{U+U_0}(-K_2\psi+\delta_2) \quad (16)$$

$$\frac{dU}{d\zeta}=\Lambda_1(U+U_0)^2K_3U+\delta_3 \quad (17)$$

where K_i construct the decision variables, and δ is given by

$$\delta = \begin{bmatrix} \delta_1 \\ \delta_2 \\ \delta_3 \end{bmatrix} = \begin{bmatrix} \frac{H}{l_c}\left(\frac{1}{\gamma_v^2}C_1 J_1 - \frac{3J_1}{4}\left(\frac{\phi+\Phi_0}{W}-1\right)+\Delta_\psi\right) \\ -\Delta_\phi \\ 0 \end{bmatrix} \tag{18}$$

3.2. Stabilizing the system at origin

The result final form of the system can be written as:

$$\begin{aligned} \dot{x} &= f_x(\zeta,\phi,\psi,U,K_i)+\delta(\zeta,J_1,\phi) \\ \dot{J}_1 &= f_{J1}(J_1,\phi,U) \end{aligned} \tag{19}$$

f_x and f_{j1} are a continuously differentiable nonlinear functions on the domain of interest D. Here, the domain of interest is a subset $D \subset R^4$ where $\psi + \Psi_0 > 0$ and the mass flow of compressors is always bounded to $\phi_{min} < \phi + \Phi_0 < \phi_{choke}$ where ϕ_{choke} is the choking value of the mass flow and ϕ_{min} is the minimum negative mass flow during deep surge (see [2] for more details). In the literature [12], there exist also other assumptions on the speed of rotor which state that $U_0 < U_0 + U < U_{max}$. $f_{J1}(J_1,\phi,\psi,U)$ is continuously differentiable in the domain D and $f_{J1}(0,0,0,0)=0$.

Lemma1 [14]

The objective of the proposed control law given in (11),(12),(13) is to find the appropriate K_i that can make the system of equations(14),(15),(16),(17) in converge to a residual subset D around the origin and are bounded. This objective can't be achieved only if

Hypothesis 1: δ is bounded ($\|\delta(\zeta,J_1,\phi)\| \le \varepsilon$.

Hypothesis 2: $\dot{J}_1 = f_{J1}(J_1,\phi,U)$ is globally input-to-state stable in D.

are verified .

3.3. Robust design

As approved in [13], the boundedness of Δ_ϕ , Δ_ψ , $\gamma_v \in [\gamma_{min},\gamma_{max}]$ and J_1 leads to the boundedness of δ as a result of hypothesis 1.

3.3.1. The input to state stability of rotating stall [14]

According to theorem 4.19 in [14], the $\dot{J}_1 = f_{J1}(J_1,\phi,U)$ is input to state stable if there is a continuous differential function $V_1 : R \to R$

$$\alpha_1(\|J_1\|) \le V_1(J_1) \le \alpha_2(\|J_1\|) \tag{20}$$

$$\frac{\partial V_1}{\partial J_1} f_{J1}(J_1,\phi,U) \le -\alpha_3(J_1) \quad \forall \|J_1\| \ge \rho(\|\phi\|,\|U\|) \ge 0 \tag{21}$$

with α_1 and α_2 are κ_∞ class functions, ρ is κ class functions and as approved in [13], the choice of Lyapunov $V_1(J_1) = \frac{1}{\rho_2} J_1^2$ with $0 < \rho_2 = \frac{3aH}{(1-m_U(U)a)W} < 1$ lead to positive function $\alpha_3(J_1)$ which proves the input to state stability of the $\dot{J}_1 = f_{J1}(J_1,\phi,\psi,U)$.

Test of Hypothesis 2: From equation (20) we obtain that:

$$\alpha_1(\|J_1\|) \le V_1(J_1) = \frac{1}{2\rho_2} J_1^2 \le \alpha_2(\|J_1\|) \quad \text{with } 0 < \rho_2 = \frac{3aH}{(1-m_U(U)a)W} < 1 \tag{22}$$

The dynamic equation (6) of non-measurable state J_1 is reformulated as

$$\frac{dJ_1}{d\zeta} = \frac{3aHJ_1}{(1-m_U(U)a)W}\left[M_1 - \frac{J_1}{4} + M_2U + M_3\phi\right] \tag{23}$$

with

$$M_1 = -\frac{\phi^2 + \Phi_0^2}{W^2} + 2\frac{\Phi_0}{W} - \frac{1}{\gamma^2}C_2\Phi_0 - G_2 < 0 \tag{24}$$

$$M_2 = G_3K_3 = \frac{2U_0\Lambda_1\Gamma(m-1)W}{3Hb}K_3 > 0 \tag{25}$$

$$M_3 = -\frac{1}{\gamma^2}C_2 + \frac{2}{W} - \frac{2}{W^2}\Phi_0 = -\frac{1}{\gamma^2}C_2 - \frac{2}{W} < 0 \tag{26}$$

From equation (22), the derivation of Lyapunov function $\dot{V}_1$

$$\frac{\partial V_1}{\partial J_1} f_{J1}(J_1,\phi,U) = J_1^2\left[M_1 - \frac{J_1}{4} + M_2U + M_3\phi\right] = M_1J_1^2 + \frac{J_1^2}{4}(-J_1 + 4M_2U + 4M_3\phi)$$

(27)

For a bounded speed U and mass flow ϕ :

$$4M_2U + 4M_3\phi < 4|M_2||U| + 4|M_3||\phi|$$

(28)

Taking $M_{23max} = max(|M_2|,M_3|)$ and $\|[U,\phi]\| = \|\upsilon\|$, the equation (28) will be written as

$$4M_2U + 4M_3\phi < 4M_{23max}\|\upsilon\| \tag{29}$$

The equation (27) has a new upper bound

$$\frac{\partial V_1}{\partial J_1} f_{J1}(J_1,\phi,U) \le M_1J_1^2 + \frac{J_1^2}{4}(-J_1 + 4M_{23max}\|\upsilon\|) \tag{30}$$

with J_1^2 is a positive definite function, $M_1 < 0$, we obtain $M_1J_1^2$ a negative define function, then provided that $-J_1 + 4M_{23max}\|\upsilon\| \le 0$ i.e. $\|J_1\| \ge 4M_{23max}\|\upsilon\|$, which yields

$$\frac{\partial V_1}{\partial J_1} f_{J1}(J_1,\phi,U) \le M_1J_1^2 \quad \forall\|J_1\| \ge 4M_{23max}\|\upsilon\| \ge 0 \tag{31}$$

The equation (31) leads to the equation (21) (Theorem 4.19 [14]), this completes the test of hypothesis 2.

3.3.2. The Robust stability of closed loop

The Lyapunov like function gives a sufficient condition for input to state robust stability. The notion of input to state stability defined for the global case where the initial state and the input can be arbitrarily large [14].

Proof of Lemma 1:

Let $V_2(\upsilon) = \frac{1}{2}\upsilon^T\upsilon$ the Lyapunov candidate definite positive function of υ then:

$$\dot{V}_2(\upsilon) = \upsilon^T\dot{\upsilon} = -K_1\phi^2 + \delta_1\phi + \frac{\Lambda_2}{(U+U_0)}(-K_2\psi^2 + \delta_2\psi) - \Lambda_1(U+U_0)^2K_3U^2$$

$$\le -K_1\phi^2 + \|\delta_1\|\phi + \frac{\Lambda_2}{(U+U_0)}(-K_2\psi^2 + \|\delta_2\|\psi) - \Lambda_1(U+U_0)^2K_3U^2$$

(32)

The verification of the two hypotheses 1 and 2, stats that the robust state feedback control (u_1,u_2,u_3) given in (11,12,13) governs the system states to a neighborhood of the origin and are bounded, for

$$-K_1\phi^2 + \|\delta_1\|\|\phi\| + \frac{\Lambda_2}{(U+U_0)}(-K_2\psi^2 + \|\delta_2\|\|\psi\|) - \Lambda_1(U+U_0)^2K_3U^2 < 0 \tag{33}$$

The equation (33) is strictly negative, implies that $\dot{V}_2(\upsilon) \le -W_3(\upsilon)$, where $W_3(\upsilon)$ is a continuous positive definite function [14]. According to theorem 4.19, considering the bounded uncertainties $\|\delta(\zeta, J_1, \upsilon)\| \le \varepsilon$ (from hypothesis 1), and the application of theorem 4.18 [14] show that in a finite time ζ_0, it exist a positive η such that: $\|\upsilon\|_2 \le \eta\varepsilon \ \ \forall\ \zeta \ge \zeta_0$, the smallest η can guaranteed by the optimal choice of K_i subjected to robustness equ. (33).

The input to state stability of the non-measured state $\dot{J}_1 = f_{J1}(J_1, \phi, U)$ leads to:
$\|J_1(\zeta)\|_2 \le \beta\left(\|J_1(0)\|_2, \zeta - \zeta_0\right) + \gamma\left(sup\|\upsilon(\zeta)\|_2, \zeta \ge \zeta_0\right) \le \beta\left(\|J_1(0)\|_2, \zeta - \zeta_0\right) + \gamma(\eta\varepsilon)$ Where β and γ are class $\kappa\mathcal{L}$ and class κ functions, respectively. Therefore, the ultimate bound of $\|J_1, \zeta\|_2$ rotating stall can be expressed as $\|J_1(\zeta, \upsilon)\|_2 \le \eta\varepsilon + \varepsilon + \gamma(\eta\varepsilon)$. This proves that the proposed control converge the state variables to a neighborhood of the origin. This completes the proof of lemma1.

3.4. Adapted Linear Matrix Inequality for the robust control design

The linear programming is a convex optimization used to find the optimal *Ki* parameters subjected to robust stability condition $\dot{V}_2(\upsilon) < 0$. The optimization problem being written as follows,

$$\begin{aligned} &Minimization\ of\ K_i \\ &Subjected\ to \\ &(a) \quad -K_1\phi^2 + \|\delta_1\|\phi < 0 \\ &(b) \quad \frac{\Lambda_2}{(U + U_0)}(-K_2\psi^2 + \|\delta_2\|\psi) < 0 \\ &(c) \quad -\Lambda_1(U + U_0)^2 K_3 U^2 < 0 \\ &(d) \quad K_i > 0 \end{aligned} \tag{34}$$

For all $\zeta > 0$, the proposed control conception leads to feasible solution K_i for each constraint separately. For a bounded ϕ, ψ, δ_1 and δ_2, the condition (a) lead to the inequality $-K_1 + \frac{\|\delta_1\|}{\|\phi\|} < 0$ for a feasible positive parameter $K_1 > \frac{\|\delta_1\|}{\|\phi\|}$, the condition (b) lead to inequality $-K_2 + \frac{\|\delta_2\|}{\|\psi\|} < 0$ for a feasible positive parameter $K_2 > \frac{\|\delta_2\|}{\|\psi\|}$, and the condition (c) leads to inequality $-\Lambda_1(U + U_0)^2 K_3 < 0$ for all feasible positive parameter K_3. The optimization problem (34) is converted to a feasible convex optimization under Linear Matrix Inequality formulation [16]:

$$\begin{aligned} &Minimization\ of\ K_i \\ &Subjected\ to \\ &-K_1 + \frac{\|\delta_1\|}{\|\phi\|} < 0 \\ &-K_2 + \frac{\|\delta_2\|}{\|\psi\|} < 0 \\ &-\Lambda_1(U + U_0)^2 K_3 < 0 \\ &K_i > 0 \end{aligned} \tag{35}$$

The interior point algorithm used to solve equation (35) is known as the most efficient algorithms used for solving LMIs that arise in robust control [16].

4. CONSTRAINED GENETIC ALGORITHM OPTIMIZED NON-LINEAR ROBUST CONTROL

The genetic algorithm is a heuristic approach to solving a non-linear optimization problem, which is essentially based on the theory of natural selection, the process that drives biological evolution. In all global search problem, there is an optimization problem of maximizing or minimizing an objective function $f(z)$ for a given space x of arbitrary dimension [21],[23],[26]. In this section, the design procedure of GA Optimized non-linear controller is presented. In this research, Constrained Genetic Algorithm (CGA) is used to design an optimum robust controller in order to reach the robust behavior of a variable speed axial compressor (VSAC) in gas turbine process. The formulation of an optimized controller involves four tasks [21], begins with the choice of control law architecture and identifying underlying controller parameters, the second is to identify the constraints associated. In this work, the constraints represent robustness criteria of a non-linear control, variable speed instabilities and certain actuators limits. The third task in the formulation procedure is to find the objective function in terms of controller parameters and other problem parameters. The final task of the formulation procedure is to set the minimum and the maximum bounds on each controller parameters [21,22]. The robust stability condition (33) is equivalent to

$$-\frac{1}{2}K_1\phi^2-\frac{\Lambda_2}{2(U+U_0)}K_2\psi^2-\Lambda_1(U+U_0)^2K_3U^2-\left(\frac{1}{2}K_1\phi^2-\|\delta_1\|\phi+\frac{\Lambda_2}{2(U+U_0)}\left(K_2\psi^2-\|\delta_2\|\psi\right)\right)<0 \quad (36)$$

Thus, finding that provides a bound on $\dot{V}_2(\upsilon)$ can be done by solving a feasible optimization problem (37):

$$-\frac{1}{2}K_1\phi^2-\frac{\Lambda_2}{2(U+U_0)}K_2\psi^2-\Lambda_1(U+U_0)^2K_3U^2-\left(\frac{1}{2}K_1\phi^2-\|\delta_1\|\phi+\frac{\Lambda_2}{2(U+U_0)}\left(K_2\psi^2-\|\delta_2\|\psi\right)\right)\le-\frac{1}{2}K_1\phi^2-\frac{\Lambda_2}{2(U+U_0)}K_2\psi^2-\Lambda_1(U+U_0)^2K_3U^2 \quad (37)$$

For all $\zeta>0$ and $K_i>0$, the feasibility of (36) is guaranteed since $-\frac{1}{2}K_1\phi^2-\frac{\Lambda_2}{2(U+U_0)}K_2\psi^2-\Lambda_1(U+U_0)^2K_3U^2$ is a negative definite function [14]. Moreover, it can be optimized over the positive K_i by searching for the smallest bound (minimization of a $f(K_1,K_2,K_3)$), imply clearly a high feedback gain. The optimization problem being written as follows:

$$\begin{aligned}&Minimization\ f(K_1,K_2,K_3)=-\frac{1}{2}K_1\phi^2-\frac{\Lambda_2}{2(U+U_0)}K_2\psi^2-\Lambda_1(U+U_0)^2K_3U^2\\&\quad Subjected\ to\\&\quad(a)\quad-\frac{1}{2}K_1\phi^2+\|\delta_1\|\phi<0\\&\quad(b)\quad\frac{\Lambda_2}{2(U+U_0)}(-K_2\psi^2+\|\delta_2\|\psi)<0\\&\quad(c)\quad-\Lambda_1(U+U_0)^2K_3U^2<0\\&\quad(d)\quad K_i>0\\&\quad(e)\quad\Lambda_1(U+U_0)^2K_3U^2+\delta_3\le\gamma_{acc}\\&\quad(f)\quad c(\phi+\Phi_0)^2-K_3U\le\gamma_{torque}\end{aligned} \quad (38)$$

The aim of constraints (a),(b) and (c) is to guarantee the stability of the closed loop in the presence of the system uncertainties and non-linearity. As demonstrated in section 2, the speed transition affects the stability of compression system and physical constraints on control efforts CCV and throttle. For that reason, we introduced a new key constraint (e) and (f) on turbine acceleration and torque, called Variable Speed instabilities

constraints. The appropriate choice of γ_{acc} and γ_{torque}, yields to achieve a better performances in terms of control dynamics, and intended to eliminate the effect of speed transition. The procedure of the proposed genetic algorithm in this work is given below [24],[23]:

a) Generate randomly a population of parameter strings to form primary population. The population number of each generation is assumed 40.

b) Calculate the fitness function as given in (38) for each individual in the population.

c) Choose parents by applying the Roulette wheel as selection function.

d) Apply crossover function to parents in order to create next generation. 0.8 is assumed as crossover fraction.

e) Apply mutation function on new population. The adapt feasible function is used in order to generate only points that are feasible with respect to linear and bound constraints [23].

f) Compute the children and parents fitness.

g) A variety of constraints-handling methods for genetic algorithms have been developed in the last decades, the two most of them can be classified as penalty function and multi-objective optimization concept [20,23]. In this work, the used concept to constraints-handling is the penalty function. The concept of penalty function is if the individual is infeasible, the penalty function is the maximum fitness function among feasible members of the population, plus a sum of the constraint violations of the (infeasible) individual, in the case of a feasible individual, the penalty function is the fitness function [20].

h) If the stopping criteria satisfied, optimization will stop, otherwise; return to step (c). The number of iterations is used as the stopping criteria and the maximum value of it is assumed as 150. An appropriate choice of parameters used for genetic algorithms performed in the present study are given in table 1.

Table 1.Parameters used for genetic algorithm

Parameter	**Function or Value**	**Parameter**	**Function or Value**
Population size	40	**Fitness function**	Equation (38)
Maximum number of generations	150	**Constraints-handling methods**	Penalty function
Type of selection	Roulette wheel	**Type of mutation:**	adapt feasible
Type of crossover	Intermediate	**Crossover Ration**	0.8

5. NUMERICAL SIMULATIONS

For the purpose of optimization (35) and (38), routines from Mathworks robust control toolbox and global optimization toolbox are used respectively. In this work, we used the feasibility solver based on Nesterov and Nemirovski's Projective Method to solve linear matrix inequality [16], and penalty constrained-handling genetic algorithm optimization [23]. As shown previously, the objective function comes from time domain simulation of gas turbine model. The relevant parameters of the system model are given in table 2. To conduct the simulations tests, two types of perturbations are applied to the system denoted by $\phi_d(\zeta)$ and $\psi_d(\zeta)$ are considered as mass flow and pressure disturbances respectively and $d_\phi(\zeta)$, $d_\psi(\zeta)$ represent the uncertainty of the compressor map and throttle characteristics.

Table 2. Numerical values used in simulations

Symbol	**Value**	**Symbol**	**Value**	**Symbol**	**Value**
W	0.25	$\phi_d(\zeta)=\psi_d(\zeta)$	$0.01\sin(0.2\zeta)$	l_E	8
H	0.18	l_i	2	c	0.7
μ	0.01	d_ϕ	−0.05	ψ_{c0}	0.3
b	96.17	d_ψ	0.02	a	0.3
m	1.75	Λ_1	2.1685e-4	R	0.1
l_c	3	Λ_2	0.0189	a_s	340

In the following time-domain simulations, the control of rotor speed without surge and rotating stall control is called Open Loop, whereas, simultaneous speed and surge/rotating stall control is called closed-loop. Here, we are interested to make the system working inside a constrained stabilizable subset $\Pi \subset R3$, $0 < \psi + \Psi_0 < \Psi_c(\Phi)$ where $\Psi_c(\Phi)$ is the compressor map. The mass flow of compressors is always limited to $\phi_{min} < \phi + \Phi_0 < \phi_{choke}$ where ϕ_{choke} is the choking value of the mass flow and ϕ_{min} is the minimum negative mass flow during deep surge (see [2] for more details). The effort signals are limited to physical constraints, effort signals u1 pressure rise through CCV valve subject to $max|u_1(\zeta)| \le max\Psi(\zeta)$, u_1 throttle valve opening gain (0: fully closed, 1: fully open) subject to $0 < u_2 < 1$, u_3 turbine torque respect the turbine limits. At ζ=0, the controller is activate and closes the loop. Examining the time response manifested in figure 2 and figure 3 for the three proposed controllers LMI On-Line (LMI-on), LMI Off-Line (LMI-off), genetic algorithm off-Line (GA), we found that the system dynamic in closed loop stay close to effective pressure rate and mass flow point under the effect of the start-up speed variation, uncertainties and perturbations.

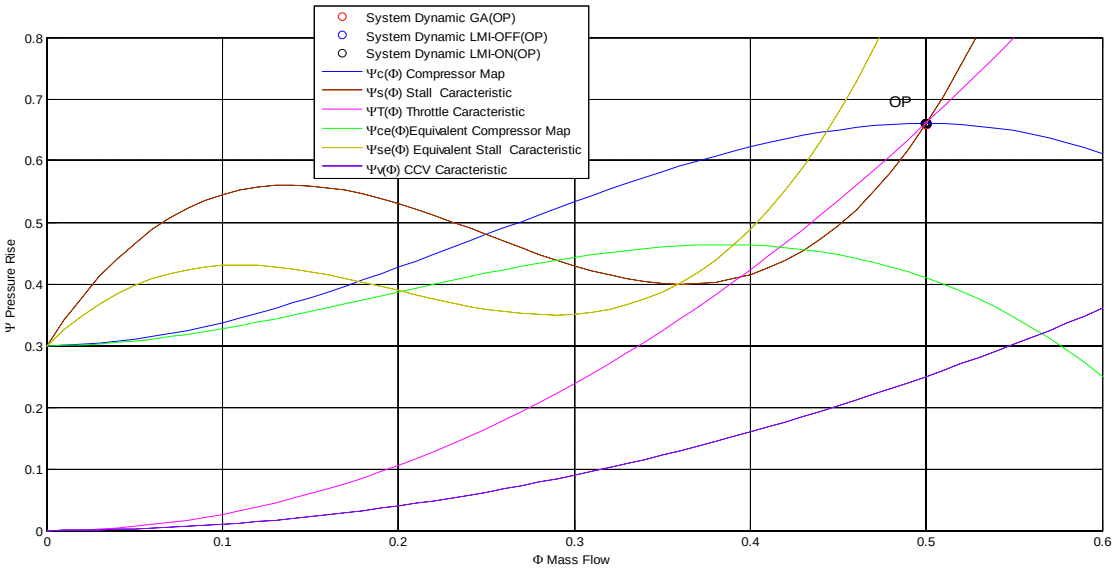

Figure 2. Closed loop System Map.

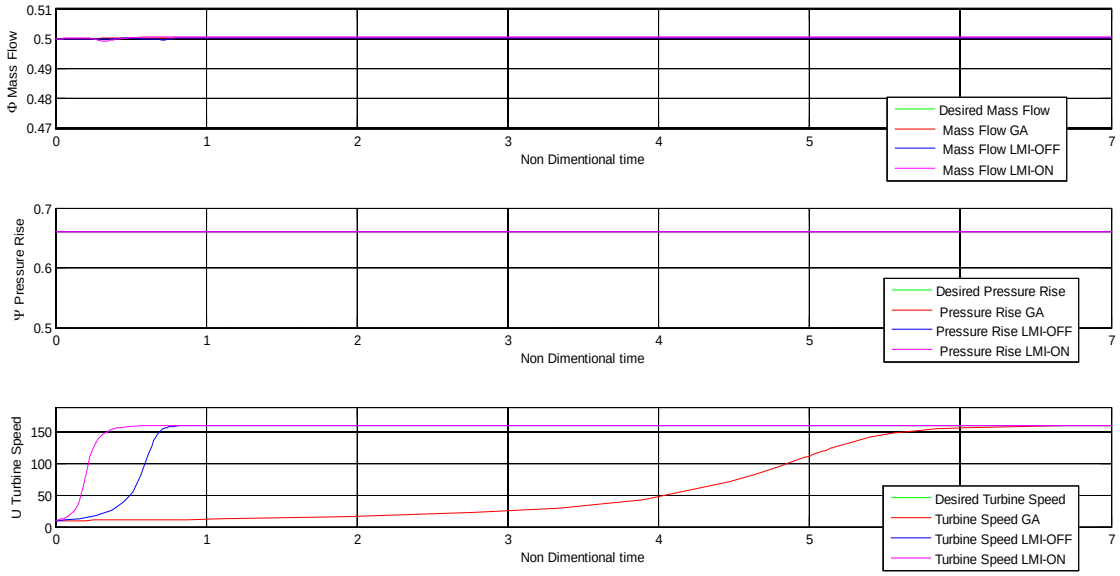

Figure 3. Output dynamic in closed Loop.

In figure 4 and table 3, it can be observed that the proposed genetic algorithm design provide a control effort signal inside the physical constraints limits, on the other hand, the control effort provided by LMI-on and LMI-off controller exceeds the physical limits of the CCV pressure rate , and throttle valve opening, which can causes the actuators saturation. It immediately damps out rotating stall (Fig. 5) and as illustrated in [10] the throttle should be turned down in order to add some resistance to the system when the flow change is positive and the pressure change rises is not negative.

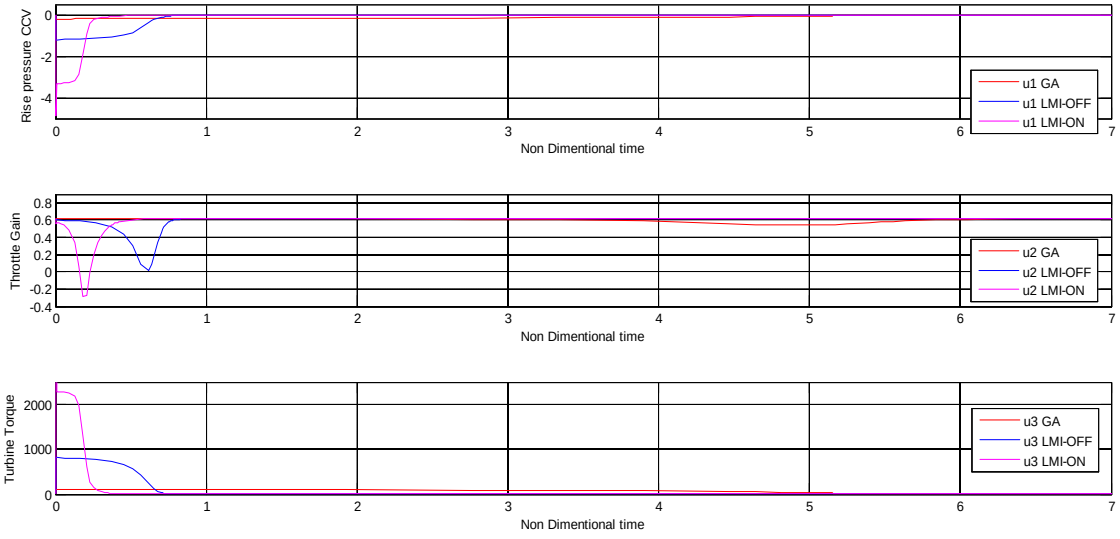

Figure 4**.** Control effort Dynamic in Closed Loop.

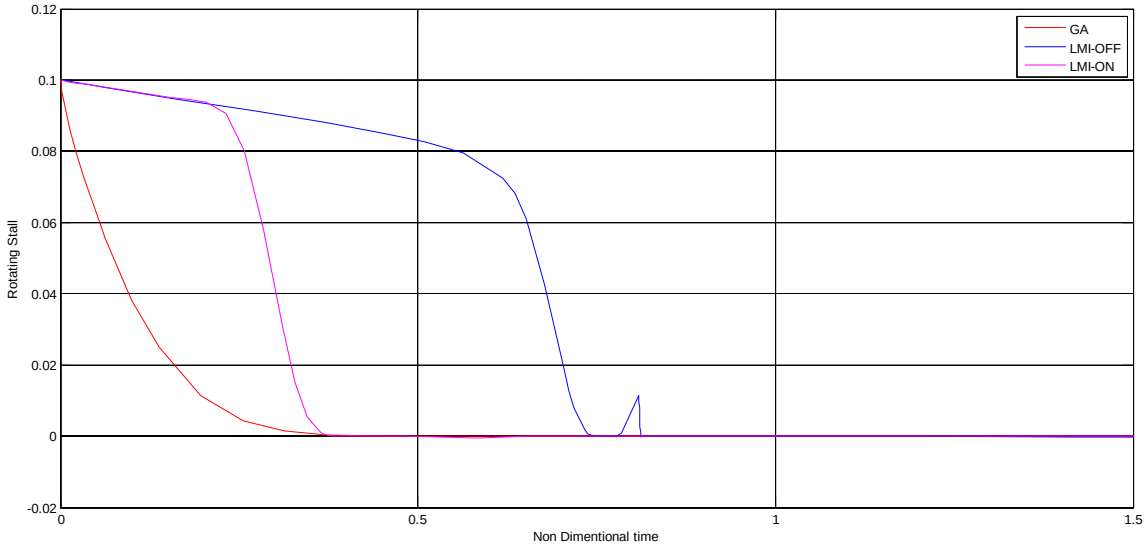

Figure 5. First Harmonic of Rotating Stall.

By investigating the results summarized in table 3, and highlighting the major difference between two controllers with the best performances, GA is an off-line optimization while LMI-on is an on-line optimization, this it will give the advantage to GA whose computation time in real-time application will not occur.

Table 3. GA and LMI results obtained for simulation 1

	GA		**LMI-ON**		**LMI-OFF**	
	Max	Min	Max	Min	Max	Min
u_1	0	-0.182	0	-4.885	0	-1.172
u_2	0.616	0.541	0.616	-0.28	0.615	0.029
u_3	99.445	0.175	3385	0.175	812.892	0.173
	Rejection time		Rejection time		Rejection time	
J	0.4		0.4		0.81	

As reported in [2], for the low speeds the system goes to rotating stall and for high speeds, it develops deep surge. In the proposed second simulation, we consider the case of low speed (35m/s) operation and demonstrate the capacity of the proposed controllers to reject the perturbations and guarantee the stability of the system inside a constrained stabilizable subset $\Pi \subset R3$. From figure 6 and figure 7, we have noted the capacity of three proposed controllers to stabilize the system in close to second operating point OP2 (Low Speed), as well as the incapacity of LMI-off to attenuate the effect of perturbation $\psi_d(\zeta) = 0.01 sin(0.2\zeta)$.

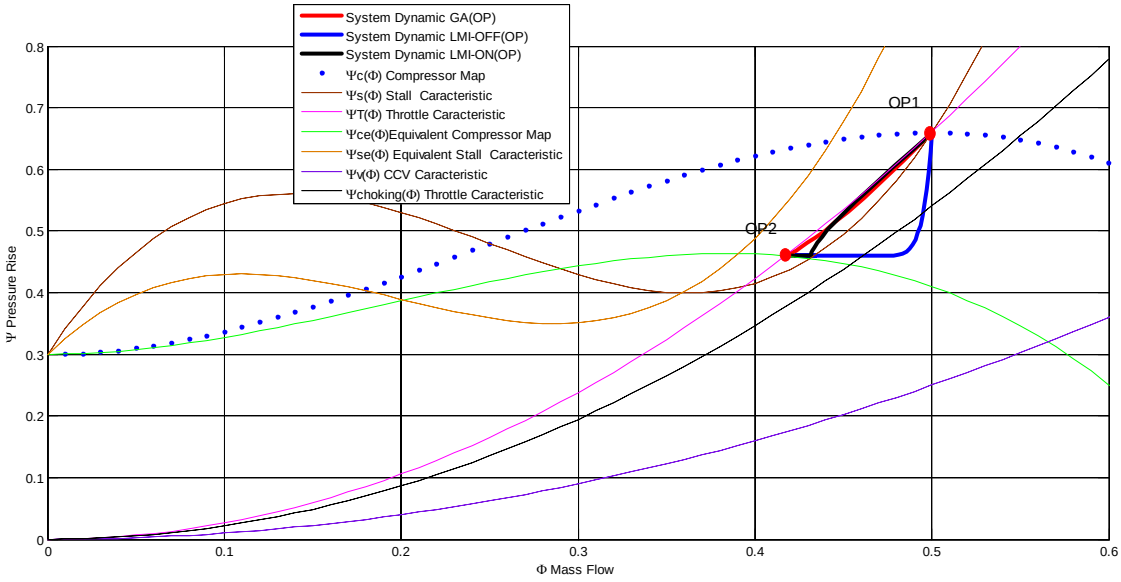

Figure 6. Closed loop system map (Low Speed).

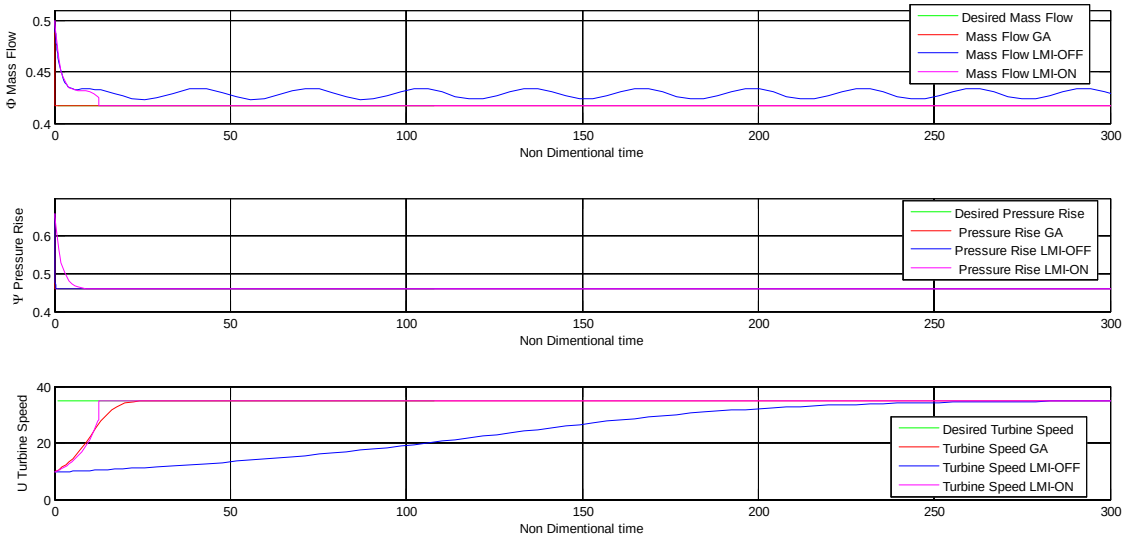

Figure 7. Output dynamic in closed loop.

Consequently in figure 8 and table 4, the LMI Off-Line controller provides an alternated effort signal, and LMI On-Line controller presents a robust stability and accepted time performances, in the detriment of control signal feasibility (pick signal), can cause mechanical damage.

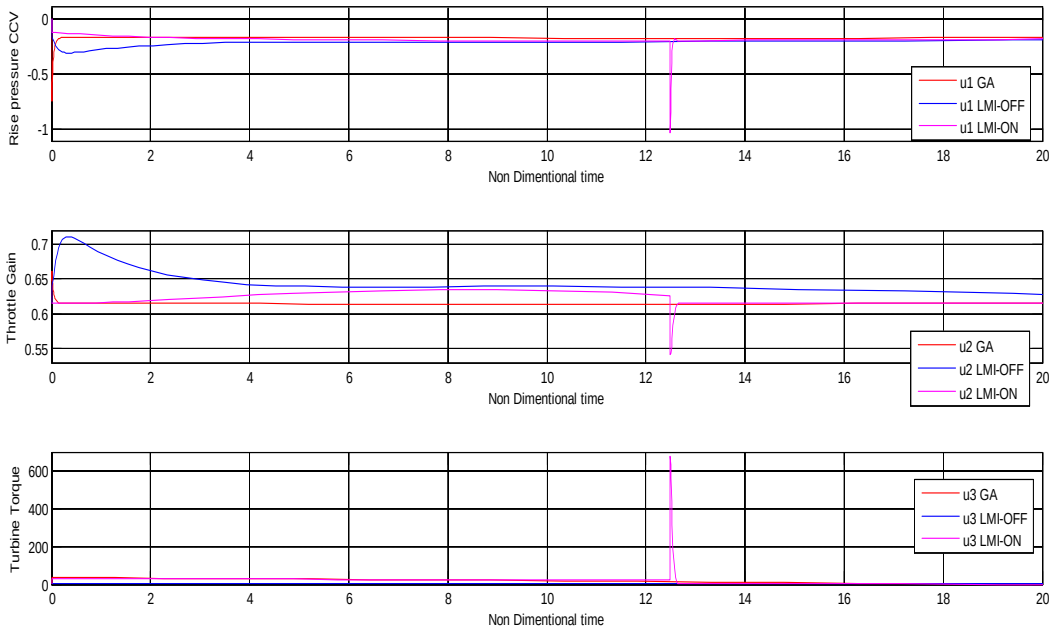

Figure 8. Control effort dynamic in closed Loop.

Concerning the rotational stall, vanishing time is satisfactory since the dimensional time t=ζR/Ud with R/Ud< 1 (Fig. 9).

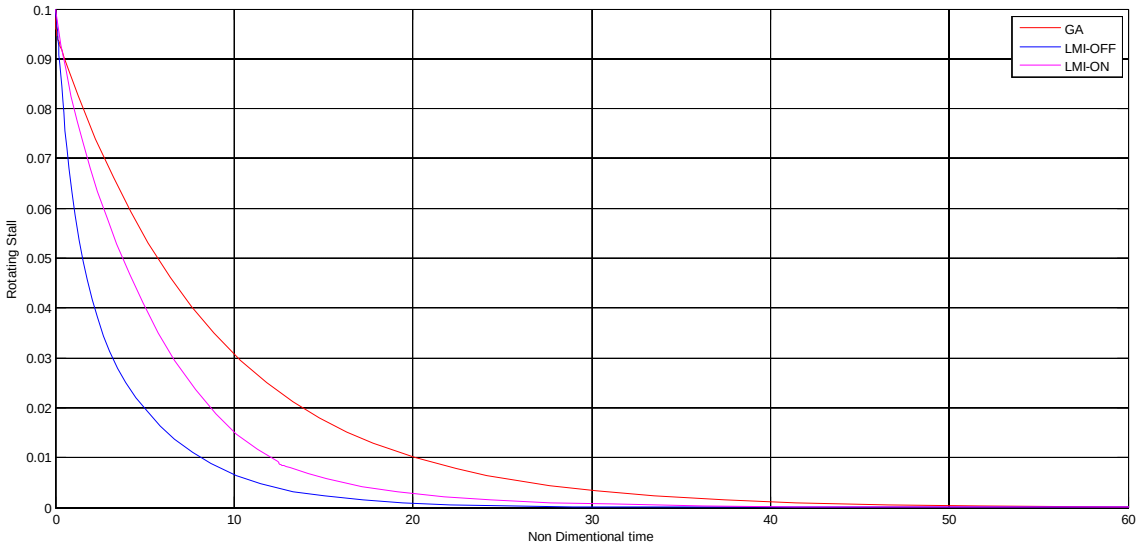

Figure 9. First Harmonic of Rotating Stall.

Additionally to the advantages of GA controller cited before regarding the table 3, table 4 proves that the combination of control parameters and objective function involved in this optimization technique, and the appropriate selection of these is a key point for feasibility and success in different operating conditions (Simulation 1 and 2).

Table 4. GA and LMI results obtained for simulation 2

	GA		**LMI-ON**		**LMI-OFF**	
	Max	Min	Max	Min	Max	Min
u_1	0	-0.18	0	-1.05	0	-0.312
u_2	0.659	0.612	0.634	0.542	0.71	0.612
u_3	34	0.121	646.833	0.044	3	0.121
	Rejection time		Rejection time		Rejection time	
J	44		43		36	
	Response time		Response time		Response time	
U	9		12.75		262	

For the completeness of the proposed controllers compared to the achievement in [28], [30],[31], this study investigated a review on the bifurcation diagrams, which formed a novel key track that involved parameters of speed dynamics can modify the transient response of the model. Here, we test this track by performing a set of time-domain simulations. Among the model parameters, the desired speed and the acceleration rate directly modify the speed dynamics. The initial speed and different operating points (from OP1 to OP2) are other key factors which determine the range of speed variations and changes the system trajectories. Furthermore, we include the constraints on acceleration rate and throttle gain as the two main bifurcation parameters of the model to make this study novel. In addition to the mathematical simplicity (compared to controllers in [28],[30],[31]), the performances of the GA optimized controller in figure 6 and figure 8 make the proposed design very promising.

6. CONCLUSION

This paper proposes a dedicated non-linear robust controllers for the studied model, which combines the advantages in terms of robustness, mathematical simplicity (compared to sliding mode control in references [28],[30] and [31]), the good convergence speed of constrained Genetic Algorithm.

The proposed approach is applied to gas turbine subjected to two distinct aerodynamic instabilities rotating stall and surge, which are associated with bifurcation. MATLAB Simulink platform is used to compare and check the three proposed controllers based on the same framework, to deal with non-linearity (Bifurcation), instabilities (surge and rotating stall) in a special operating conditions (Design Constraint, Physical limits). Overall, the simulation results indicate the capacity of the genetic algorithm to tackle with this kind of problem, due to constraint-handling in restricted solution area, instead to the LMI approach.

The contribution of this paper is to incorporate the non-linear constraints on compressor acceleration and turbine torque, and the appropriate choice of these is a key for a feasible solution and accepted performances. Additionally, problem reformulation and robust objective function are involved in GA optimization, and appropriate selection of genetic parameters is another contribution. The achieved robust performance of optimized GA controller in addressing to system uncertainties and disturbances shows its great applicability in a real prototype.

Nomenclature

Φ : Annulus averaged mass flow coefficient of axial velocity
Ψ : Total to static pressure rise coefficient
J_n : The n mode squared amplitude of rotating stall
U : Rotor tangential velocity at mean radius
U_d : Desired constant velocity
B : Greitzer's B-parameter
γ_T : Throttle Gain
γ_v : Close Coupled valve gain
ζ : Non-dimensional time
t : Dimensional (actual) time
R : mean compressor radius
$\Psi_c(\Phi)$: Compressor characteristic
$\Psi_s(\Phi)$: Stall characteristic
H, W, ψ_{co} : Parameters of Compressor characteristic
Γ_c : Non-dimensional Compressor torque
Γ_t : Non-dimensional Turbine torque
l_c, l_i, l_E : Effective flow passage non-dimensional length of the compressor , Inlet duct and exit duct respectively.
m : Compressor duct flow parameter
β_1, β_2 : Constant blade angles at rotor input
a : Reciprocal time lag parameter of the blade passage
a_s : Sonic velocity
μ : Viscosity
Λ_1, Λ_2 :Constants in Greitzer model
b : Constant $U = bB$
$d_\phi, d\psi$: Mass flow and pressure uncertainty
Φ_d, Ψ_d :Time varying and mass flow pressure disturbance
K_s : Gain defining the rate of the acceleration
K_i :Controller parameters

REFERENCES

[1] Gravdahl J.T., Egeland O., 1997. Moore-Greitzer Axial Compressor Model with Spool Dynamics, Proceedings of 36th IEEE Conf. on Decision and Control, CA, USA, 4714-4719.

[2] J.T. Gravdahl J.T., 1998. Modeling and control of surge and rotating stall in compressors, doctoral diss., Department of Engineering Cybernetics, Norwegian University of Science and Technology, Trondheim.

[3] Sari G., O.Akhrif O. & Saydy L., 2011. Qualitative Analysis of an Axial Compressor Model with Non-constant Speed, Proceedings of ASME 2011 Power Conference, Denver, Colorado, USA, 515-524.

[4] Sari G., Akhrif O., & Saydy L., 2012. The impact of speed variation on the stability of variable speed axial compressors at efficient operating points", Proceedings of American Control Conference, Montréal, Canada.

[5] Liaw D., Ren S. M., & Chang S., 2008. A feedback linearization design for compressor's surge control in Industrial Technology, Proceedings of ICIT 2008. IEEE International Conference,1-6.

[6] Dhooge A., Govaerts W. & Kuznetsov Y. A., 2003. MATCONT: A Matlab Package for Numerical Bifurcation Analysis of ODEs, ACM Transactions on Mathematical Software, Vol. 29(1), 141-164.

[7] Seydel R., 2010. Practical Bifurcation and Stability Analysis, Interdisciplinary Applied Mathematics, 3 (5), Springer Science+Business Media, 303-353 .

[8] Zaiet C., Akhrif O. & Saydy L., 2006. Modeling and Non Linear Control of a Gas Turbine, Proceedings of International Symposium on Industrial Electronics, Canada, 2688-2694.

[9] Chen Z., Xu J., 2013. Nonlinear feedback control for rotating stall and surge of an axial flow compressor, Journal of Vibration and Shock, 32, 106-120.

[10] Lin S., Yang C., Wu P., & Z.Song, 2014. Active surge control in variable speed axial compressors, ISA Transactions, Elseiver, Vol. 53 (5), 1389-1395.

[11] Xiao L., Zhu Y., 2012. Compressor active surge controller design based on uncertainty and disturbance estimator, Proceedings of 10th World Congress on Intelligent Control and Automation WCICA, Beijing, China, 2908-2912.

[12] Ghanavati1 M., Salahshoor K., Motlagh M.R.J., Ramazan A. & Moarefianpour A., 2018. A novel combined approach for gas compressors surge suppression based on robust adaptive control and backstepping, Journal of Mechanical Science and Technology, Vol. 32 (2), pp 823-83.

[13] Sari G., 2014, Model analysis and nonlinear control of air compressors, doctoral diss., Montreal University, Canada.

[14] Khalil H.K., Nonlinear Systems, 2002. 3rd ed.Prentice Hall Upper Saddle River.

[15] Chen P.C., Chiang C.H. & Liu J.C,2009. The input/output constarained control for V/STOL aircraft dynamics under a descriptor system formulation, Journal of Aeronautic and aviation, Series A, Vol. 41(1), 43-52.

[16] Boyd S.,1994. Linear Matrix Inequalities in System and Control Theory, Society for Industrial and Applied Mathematics, 15 Philadelphia: Siam ,7-47.

[17] Sheng H., Huang W., Zhang T., & Huang X., 2014. Robust Adaptive Fuzzy Control of Compressor Surge Using backstepping , Arab Journal of science engineering, Vol. 39, 9301–9308 .

[18] Sheng H., Huang W., & Zhang T., 2017, Output Feedback Control of Surge and Rotating Stall in Axial Compressors, Asian Journal of control ,19(2), 599-565.

[19] Bitikofer C., Schoen M.P., 2017, Characteristic Moore-Greitzer Model Parameter Identification for a one stage Axial Compressor System, Proceedings of American Control Conference , Seattle, USA, 164-169.

[20] Deb K., 2000, An efficient constraint handling method for genetic algorithm, Computer methods in applied mechanics and engineering, Elseiver, Vol. 186, 311-338.

[21] Deb K., 2012. Optimization for Engineering Design: Algortithms and Examples, 2nd ed. PHI Learning Private Limited.

[22] Khan A.A., Mir R.N., 2017, Optimization of Constrained Function Using Genetic Algorithm, Computer Engineering and Intelligent System ,Vol. 8(2), 11-15.

[23] Kramer O., 2010. A Review of Constraint-Handling Techniques for Evolution Strategies, International Computer Science Institute, USA, 1-11.

[24] Panda S., Padhy N.P., 2008. Comparison of particle swarm optimization and genetic algorithm for FACTS-based controller design, Elsevier Applied Soft Computing, Vol. 8, 1418–1427.

[25] Yakhelef Y., Boulouh M., 2014. Performance improvement of Minmax optimized PI Controller based DC drive system with actuator stauration, Control and intelligent systems journal, Vol. 42(4), 271-278.

[26] Houck C.R., Joines J. & Kay M., 1995. A Genetic Algorithm for Function Optimization: A Matlab Implementation, NCSU-IE TR 95-05, North Carolina State University.

[27] Parvaneh H.,.Dizgah S.M, Sedighizadeh M., & Ardeshir S.T. ,2016. Load Frequency Control of a Multi-Area Power System by Optimum Designing of Frequency-Based PID Controller Using Seeker Optimization Algorithm, Proceedings of 6th Conf on Thermal Power Plants, CTPP, Iran University of Science and Technology, Tehran, Iran, 52-57.

[28] Debbah A, Kherfane H. & Kerboua A., 2016. Using robust sliding mode controller to improving the aerodynamic performance of a gas turbine, Proceedings of 4th Internatinal seminar on new and renewable energies SIENR, Ghardia, Algeria, 1-6

[29] Liu X., Xi H., 2014. Stability and optimality algorithm for neutral delay systems with actuator saturation, Control and Intelligent Systems, Vol. 42(3), 201-209.

[30] Debbah A., Kherfane H., 2018, GA/PSO robust sliding mode control of aerodynamics in gas turbine, Acta Universitatis Sapientiae Electrical and Mechanical Engineering, Vol. 10(1), 42-66.

[31] Debbah A., Kherfane H & Kerboua A., 2018. Control of gas turbine aerodynamics via an Optimized robust sliding mode design, Proceedings of Third International Conference on Technological Advances in Electrical Engineering (ICTAEE'18),Skikda,Algeria,1-